Simulated Fewer-Angle SPECT/CT Imaging Protocol for Parathyroid Adenoma

Jennifer B. Ficke[1], Nora L. Watson[2], Derek J. Stocker[1], Kevin E. Schlegel[1], Maya C. Sahajwalla[1], and Chad C. Adams[3]

[1]*Department of Radiology, Walter Reed National Military Medical Center, Bethesda, Maryland;* [2]*Department of Research Programs, Walter Reed National Military Medical Center, Bethesda, Maryland; and* [3]*Department of Radiology, Eisenhower Army Medical Center, Augusta, Georgia*

A new SPECT/CT protocol for parathyroid imaging detailing fewer image-angle acquisitions (fewer-angle SPECT/CT [FASpecT/CT]) was evaluated for identification of parathyroid adenoma. The motivation for validating this protocol was to be able to use it in the future to decrease patient imaging time in our clinic. **Methods:** This was a retrospective review of existing data performed as a simulated case control study evaluating 50 parathyroid SPECT/CT scans acquired using the standard 60-stop protocol and the tested 15-stop FASpecT protocol acquired using angular sampling software. Agreement on the final interpretations between imaging methods was evaluated using the McNemar test and the Cohen κ. Interrater reliability among the 3 readers was described for each method using the Fleiss κ interpreted as in the strength-of-agreement guidelines by Landis and Koch. **Results:** Of the 50 evaluated images, 45 (90%) had concordant final image interpretations between imaging methods. The sensitivity of FASpecT/CT relative to SPECT/CT was 17 of 19 (89.5%; 95% CI, 66.9%–98.7%), and the specificity was 28 of 31 (90.3%; 95% CI, 74.2%–98.0%). Additionally, there was statistically significant substantial agreement between protocols and among readers for each protocol. **Conclusion:** Adequate diagnostic-quality SPECT/CT images can be acquired using significantly fewer imaging stops given advances in camera quality and processing algorithms such as iterative reconstruction.

Key Words: SPECT/CT; FASpecT; parathyroid adenoma

Several imaging modalities are available to localize parathyroid adenomas, including ultrasound, multiphase contrast-enhanced CT (also known as 4-dimensional CT), MRI, and parathyroid scintigraphy. Of these, scintigraphy is the most effective modality for localizing cervical and ectopic adenomas in the neck and mediastinum (*1*). Additionally, the diagnostic value of separately acquired fused SPECT and CT images for localization of an ectopic parathyroid adenoma was first reported in 2002 by Rubello et al. (*2*). Multiple subsequent larger studies demonstrated the ability of SPECT/CT to localize cervical parathyroid adenomas (*3–7*). Minimally invasive surgical management of parathyroid adenomas relies on precise localization accomplished with SPECT/CT (*8,9*). Another notable benefit is the ability to differentiate pathologic uptake from nonpathologic uptake such as external contamination. As such, SPECT/CT is a valuable tool that brings many benefits when added to planar parathyroid scintigraphy for localization and diagnosis of parathyroid adenoma.

The primary downside of the addition of SPECT/CT to the planar parathyroid protocol is a significant increase in examination time. This increase can result in decreased clinic efficiency, increased likelihood of motion artifacts, and increased patient discomfort. Planar parathyroid images typically require 10 min of static acquisition both in the early and in the delayed phases for a total of 20 min. For nuclear medicine clinics performing SPECT/CT on both the early and the delayed phases of the parathyroid study using a protocol similar to our standard protocol as detailed below, each patient will require approximately 60 min of additional imaging time compared with planar imaging alone. In total, this amounts to approximately 80 min of camera time per parathyroid study. Decreasing the time spent acquiring the SPECT/CT images can help to mitigate this extended camera time. All SPECT images are acquired in multiple stops, which represent points where the dual heads of the camera stop moving every set number of degrees to acquire an image as they rotate 360° around the patient. Patient imaging time per study can be decreased by decreasing the number of image acquisition stops (by increasing the degrees between each stop) or decreasing the acquisition time at each stop. Our hypothesis stated that adequate diagnostic-quality SPECT/CT images can be acquired using significantly fewer imaging stops, without changing the acquisition time per stop, given advances in camera quality and processing algorithms such as iterative reconstruction (*10*). We refer to this technique as fewer-angle SPECT/CT (FASpecT/CT).

MATERIALS AND METHODS

This study was a retrospective review of existing data performed as a simulated case control study evaluating 50 parathyroid SPECT/CT scans performed at Walter Reed National Military Medical Center from June 2017 through March 2021. Approval was granted by the

Walter Reed Institutional Review Board, and the requirement to obtain informed consent was waived. All patients imaged on the GE Healthcare Optima SPECT/CT scanner during that period were included for analysis. Patients imaged on other cameras were excluded because those datasets could not be reprocessed using Xeleris (GE Healthcare) angular sampling. Patients were assigned to different cameras on the basis of clinic workflow and camera availability, and there were no differences in patient characteristics or study indications between those patients assigned to the Optima system and those assigned to other cameras used for this examination. For purposes of this study, standard SPECT/CT was considered to be the gold standard. Scans were performed with an Optima SPECT/CT camera with a collimator using a 140-keV photopeak and 20% window.

The FASpecT/CT protocol consists of 15 stops each lasting 25 s with a total imaging time of approximately 7 min 30 s versus the conventional SPECT/CT protocol consisting of 60 stops lasting 25 s each with a total imaging time of approximately 30 min. The Xeleris processing capability angular sampling allowed us to take the 60-stop standard SPECT/CT already performed on our last 50 parathyroid scintigraphy patients and reprocess the data using only every fourth stop to simulate a 15-stop FASpecT/CT. With this procedure, data from a fraction of the stops were selected and used to create the reconstruction. As detailed in Table 1, 15 of the original 60 stops were extracted in Xeleris and reprocessed. This approach allowed the patient to be imaged using currently accepted standard-of-care conventional SPECT/CT, which we also used as an internal reference standard to compare the performance of the derived FASpecT/CT.

Images were interpreted on Hermes Client Workstations (Hermes Medical Solutions), per the standard departmental protocol. Three masked nuclear medicine trained physicians interpreted the deidentified and randomized conventional and simulated product images as positive or negative for adenoma.

Final image interpretations for each imaging method were defined as the majority interpretation (positive vs. negative for adenoma) for the study among the 3 readers. Agreement on final interpretations between imaging methods was evaluated using the McNemar test and the Cohen κ. The sensitivity and specificity of the final interpretations using FASpecT/CT relative to SPECT/CT were reported with their 95% exact CIs. Interrater reliability among the 3 readers was described for each method using the Fleiss κ. κ-values were interpreted as in strength-of-agreement guidelines proposed by Landis and Koch (11).

RESULTS

Of the 50 evaluated images, 45 (90%) had concordant final interpretations between imaging methods. Of the 5 images with discordant interpretations, 3 were interpreted as positive by FASpecT/CT and negative by SPECT/CT, and 2 were interpreted as negative by FASpecT/CT and positive by SPECT/CT. The sensitivity of FASpecT/CT relative to SPECT/CT was 17 of 19 (89.5%; 95% CI, 66.9%–98.7%), and the specificity was 28 of 31 (90.3%; 95% CI, 74.2%–98.0%). The frequencies of paired final interpretations did not statistically differ between imaging methods (McNemar test, $P = 0.65$). Cohen κ was 0.79 (95% CI, 0.62–0.96), indicating substantial agreement (≥0.61) between methods, with confidence limits within the ranges of substantial to near-perfect agreement (≥0.81). The Fleiss κ for interrater reliability was 0.70 for FASpecT/CT and 0.65 for SPECT/CT, indicating substantial agreement among readers for each method.

All images from the 50 patients were reviewed by 3 masked nuclear medicine–trained physicians. Representative images from 2 patients are presented with a brief history (Figs. 1 and 2).

DISCUSSION

A conclusion specifically concerning the diagnostic accuracy of the FASpecT/CT protocol for parathyroid adenoma detection cannot be drawn because there is no validated gold standard in the literature. A contributing factor to the lack of a gold standard is that institutions use several different imaging modalities for parathyroid adenoma localization, including ultrasound, multiphase contrast-enhanced CT (also known as 4-dimensional CT), MRI, and scintigraphy. Although scintigraphy is the favored method, multiple acquisition protocols exist, making direct comparison difficult. This study evaluated a commonly used 60-projection/25-s-per-projection protocol and aimed to reduce acquisition times while maintaining adequate image quality. As such, for the purposes of this study, final image interpretations using the original 60-projection/25-s-per-projection protocol were considered the gold standard. Lesions detected with

TABLE 1
Simulated FASpecT/CT Acquisition and Processing Parameters Compared with Conventional SPECT/CT

Parameter	Simulated FASpecT/CT	Conventional SPECT/CT
SPECT acquisition	24° stops and total angular range of 360° with dual-head SPECT/CT camera	6° stops and total angular range of 360° with dual-head SPECT/CT camera
Acquisition time per stop	25 s	25 s
Number of stops	15	60
Total images acquired	30	120
Matrix size	128 × 128	128 × 128
Reconstruction	Iterative (OSEM)	Iterative (OSEM)
OSEM parameters	3 iterations, 30 subsets	3 iterations, 30 subsets
Postreconstruction filter	Butterworth	Butterworth

OSEM = ordered-subsets expectation maximization.
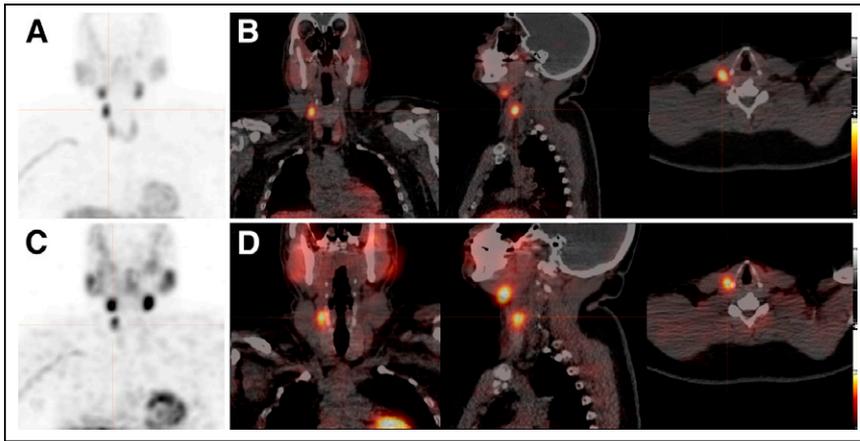
FIGURE 1. Patient 1, 55-y-old man with nephrolithiasis and laboratory-diagnosed primary hyperparathyroidism (calcium, 12.2 mg/dL; parathyroid hormone, 327 pg/mL). (A) SPECT image with 60-stop protocol. (B) SPECT/CT images with 60-stop protocol. (C) SPECT image with 15-stop protocol. (D) SPECT/CT images with 15-stop protocol. Images from left to right are coronal SPECT followed by coronal, sagittal, and axial SPECT/CT.

the FASpecT/CT protocol but not with the original standard protocol are considered false positives. Similarly, undetected lesions using the FASpecT/CT protocol were considered false negatives. There was statistically significant diagnostic agreement between simulated FASpecT/CT and standard SPECT/CT for the diagnosis of parathyroid adenoma.

There have been preliminary investigations of similar protocols in nuclear medicine using SPECT imaging with fewer sampled angles, but none, to our knowledge, have specifically evaluated parathyroid lesion detection. A study by Takahashi et al. demonstrated similar diagnostic image quality, defined as uniformity and resolution, comparing 30, 60, and 120 stops while also accounting for camera dead time. Each image had large acquisition counts and used both filtered backprojection

and iterative backprojection (ordered-subset expectation maximization and maximum-likelihood expectation maximization), with large acquisition counts specifically finding clinically relevant improvement with ordered-subset expectation maximization (*12*). This study was limited because it did not evaluate protocols using fewer than 30 stops, and the fastest evaluated method required greater than 15 min.

Phillips et al. demonstrated successful localization of focal hyperemia and inflammation associated with osteomyelitis in the spine, tendonitis in the foot and hand, and soft-tissue infection of the foot using a similar protocol with fewer stops. Specifically, the protocol dictates 6 stops at 30° (12 views) with a 3-dimensional dual camera (*13*). Each stop requires 30 s, with the whole acquisition imaging time totaling 3 min. This protocol is only recommended to be used with iterative reconstruction techniques such as ordered-subset expectation maximization because of its ability to maintain excellent image quality with a reduced number of angle samples. The researchers in this study suggested the fast acquisition protocol may be used for many other clinically relevant examinations (*13*).

The group further evaluated the 6-stop 30° dual-camera technique in a subsequent study demonstrating improved ^{131}I-NaI image quality and increased sensitivity for detection of metastatic neck and chest lymph nodes in low-count-rate images (*14*). In this study, they found that the protocol increased lesion detection in cases with low count rates and reduced the acquisition time in cases with high count rates.

To improve the sensitivity of the low-count-rate images, the acquisition times varied from 30 s to 3 min per stop, with lower count rates requiring a longer acquisition time to improve the reconstruction statistics. The total SPECT time ranged from 3 to 18 min and allowed for protocol tailoring based on the clinical scenario (*14*).

Adjusting both the number of imaging projections and the acquisition time at each projection will reduce the overall scan time. In addition to our tested decreased number of stops, a protocol using a shorter acquisition time per stop may theoretically be applied to localize lesions with high count rates. This concept of decreased acquisition times for high count rates was integrated into the 2009 European Association of Nuclear Medicine guidelines,
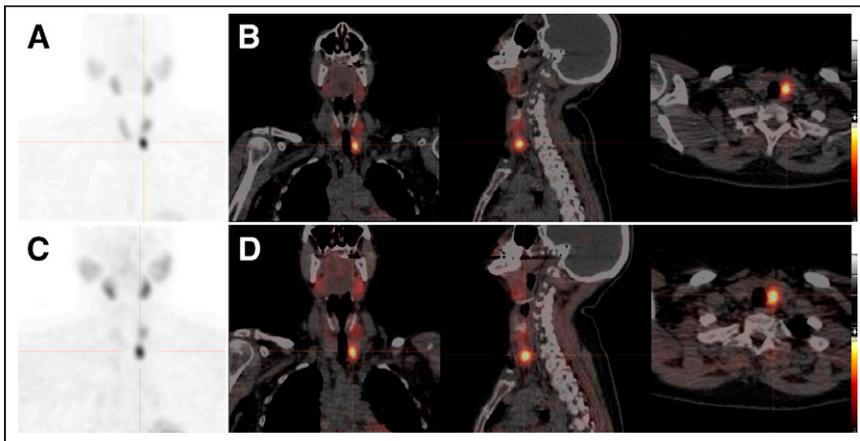
FIGURE 2. Patient 2, 53-y-old woman with osteopenia resulting in 2 recent fractures (foot and rib), constipation, and laboratory-diagnosed primary hyperparathyroidism (calcium, 11.5 mg/dL; parathyroid hormone, 97 pg/mL). (A) SPECT image with 60-stop protocol. (B) SPECT/CT images with 60-stop protocol. (C) SPECT image with 15-stop protocol. (D) SPECT/CT images with 15-stop protocol. Images from left to right are coronal SPECT followed by coronal, sagittal, and axial SPECT/CT.

which detail 120 projections every 3° with an imaging time of 15–25 s per projection. This suggests that acquisition time per stop can be reduced to 15 s while maintaining sufficient sensitivity for lesion location when using many stops (*15*). Our study was limited in that because of its retrospective nature using the Xeleris reprocessing software, it evaluated only the impact of reduced imaging stops, not a reduction in acquisition time at each stop.

These studies highlight the importance of iterative reconstruction. Detectors move around an axis of rotation acquiring images for each projection. In filtered backprojection, the information is projected back to the center of the matrix, reinforcing the center point source but ultimately creating a star artifact. Reduced counts resulting from reduced stops in the tested protocol produce an unacceptable artifact due to the greatly reduced number of sampled angles when using this method (*16*). Iterative reconstruction is thus crucial to reduce this artifact and produce acceptable image quality. Ordered-subset expectation maximization was used in this study and is the most commonly applied method of iterative reconstruction. The method models only the most important information in the data and suppresses the features most likely to be noise. There are recent studies detailing emerging improved methods of iterative reconstruction to even further increase image quality, potentially allowing for even shorter acquisition times (*17,18*).

Advancing and new camera systems additionally may reduce acquisition time secondary to their improved temporal resolution. This study was conducted using a γ-camera with a NaI(Tl) scintillation crystal. Conceptually, a scintillator converts absorbed photon energy to visible light, which is subsequently detected by photomultiplier tubes and converted to an electric signal. This signal is further processed, resulting in image production. This multistep process allows for relatively large uncertainty in the final measured signal. Additionally, determination of the interaction location within the scintillation crystal requires multiple photomultiplier tubes that need to be carefully tuned to produce signals with similar amplitude (*10*). The recent introduction of solid-state detector material such as cadmium-zinc-telluride improves on these limitations. The solid-state detector directly generates an electric signal using induced charge from photoelectric interactions and Compton scattering collected by individual anodes acting as detectors. Since each anode acts as an individual detector, there is a higher count rate performance than with traditional scintillation crystals (*10*). Theoretically, these camera advancements could be used to further reduce acquisition time, allowing for a faster protocol.

Improved processing algorithms such as ordered-subset expectation maximization allow for imaging protocols with a reduced number of stops, such as FASpecT/CT, to significantly reduce imaging time. The FASpecT/CT protocol allows for a 75% decrease in SPECT/CT imaging time when compared with conventional protocols. Naturally, the longer the scan, the more artifact is captured with cardiac and respiratory motion. The patient is also more likely to become uncomfortable and move with extended periods on the imaging table. Patient motion increases image blurring. Blur is most pronounced at focal areas of uptake at which precision is most important for diagnosis. Additionally, it can significantly reduce the accuracy of spatial alignment between nonsimultaneously acquired images such as SPECT and CT (*19*). This is especially important in small anatomic areas such as the parathyroid glands as demonstrated in this study. Decreased scan time directly relates to decreased likelihood of motion artifact and improved patient comfort and cooperation. Faster patient throughput is an additional benefit to the fast protocol, allowing for more efficient imaging centers with an increased number of daily scans and improved patient care. The benefits of this protocol have been demonstrated in blood pool imaging, infection, and thyroid cancer and can likely be applied to other types of SPECT/CT imaging (*13,14*).

CONCLUSION

There is statistically significant diagnostic agreement between simulated FASpecT/CT and standard SPECT/CT for the diagnosis of parathyroid adenoma. This new approach reduces the number of stops and decreases the image acquisition time while maintaining diagnostic image quality. This retrospective proof-of-concept study may provide justification for further prospective investigation into the use of FASpecT/CT protocols in the diagnosis of parathyroid adenoma.

DISCLOSURE

The opinions and assertions expressed here are those of the authors and do not necessarily reflect the official policy or position of Walter Reed National Military Medical Center or the Department of Defense. No potential conflict of interest relevant to this article was reported.

KEY POINTS

QUESTION: Does the FASpecT/CT protocol produce acceptable diagnostic image quality?

PERTINENT FINDINGS: There was statistically significant concordance in final image interpretations between the standard imaging protocol and the FASpecT/CT imaging protocol.

IMPLICATIONS FOR PATIENT CARE: It is acceptable to regularly use the FASpecT/CT protocol for parathyroid imaging in patient care, allowing for faster scans and increased patient comfort.

REFERENCES

1. Greenspan BS, Dillehay G, Intenzo C, et al. SNM practice guideline for parathyroid scintigraphy 4.0. *J Nucl Med Technol.* 2012;40:111–118.
2. Rubello D, Casara D, Fiore D, Muzzio P, Zonzin G, Shapiro B. An ectopic mediastinal parathyroid adenoma accurately located by a single-day imaging protocol of

Tc-99m pertechnetate-MIBI subtraction scintigraphy and MIBI-SPECT-computed tomographic image fusion. *Clin Nucl Med.* 2002;27:186–190.

3. Gayed IW, Kim EE, Broussard WF, et al. The value of ^{99m}Tc-sestamibi SPECT/CT over conventional SPECT in the evaluation of parathyroid adenomas or hyperplasia. *J Nucl Med.* 2005;46:248–252.

4. Wong KK, Fig LM, Gross MD, Dwamena BA. Parathyroid adenoma localization with ^{99m}Tc-sestamibi SPECT/CT: a meta-analysis. *Nucl Med Commun.* 2015;36: 363–375.

5. Israel O, Pellet O, Biassoni L, et al. Two decades of SPECT/CT: the coming of age of a technology—an updated review of literature evidence. *Eur J Nucl Med Mol Imaging.* 2019;46:1990–2012.

6. Vaz A, Griffiths M. Parathyroid imaging and localization using SPECT/CT: initial results. *J Nucl Med Technol.* 2011;39:195–200.

7. Vaiman M, Cohenpur M, Halevy A, et al. Low-radiation of technetium-99m-sestamibi and single-photon emission computed tomography/computed tomography to diagnose parathyroid lesions. *World J Nucl Med.* 2019;18:52–57.

8. Taubman ML, Goldfarb M, Lew JI. Role of SPECT and SPECT/CT in the surgical treatment of primary hyperparathyroidism. *Int J Mol Imaging.* 2011;2011:141593.

9. Eslamy HK, Ziessman HA. Parathyroid scintigraphy in patients with primary hyperparathyroidism: [99m]Tc sestamibi SPECT and SPECT/CT. *Radiographics.* 2008;28:1461–1476.

10. Ljungberg M, Pretorius PH. SPECT/CT: an update on technological developments and clinical applications. *Br J Radiol.* 2018;91:20160402.

11. Landis JR, Koch GG. The measurement of observer agreement for categorical data. *Biometrics.* 1977;33:159–174.

12. Takahashi Y, Murase K, Mochizuki T, et al. Evaluation of the number of SPECT projections in the ordered subsets-expectation maximization image reconstruction method. *Ann Nucl Med.* 2003;17:525–530.

13. Phillips WT, Gorzell B, Martinez R, et al. Rapid SPECT/CT blood pool imaging for more accurate localization of infection and inflammation [abstract]. *J Nucl Med.* 2017;58(suppl 1):1218.

14. Phillips WT, Kukkar V, Francis GL, et al. FASpecT/CT, a new SPECT/CT acquisition with higher sensitivity and efficiency in radioiodine thyroid cancer imaging. *Clin Nucl Med.* 2020;45:356–364.

15. Hindié E, Ugur O, Fuster D, et al. 2009 EANM parathyroid guidelines. *Eur J Nucl Med Mol Imaging.* 2009;36:1201–1216.

16. Hutton BF. Recent advances in iterative reconstruction for clinical SPECT/PET and CT. *Acta Oncol.* 2011;50:851–858.

17. van Hoorn RA, Vriens D, Postema JW, et al. The influence of SPECT reconstruction algorithms on image quality and diagnostic accuracy in phantom measurements and ^{99m}Tc-sestamibi parathyroid scintigraphy. *Nucl Med Commun.* 2014;35:64–72.

18. Davidsson A, Olsson E, Engvall J, Gustafsson A. Influence of reconstruction algorithms on image quality in SPECT myocardial perfusion imaging. *Clin Physiol Funct Imaging.* 2017;37:655–662.

19. Livieratos L. Technical pitfalls and limitations of SPECT/CT. *Semin Nucl Med.* 2015;45:530–540.